Numerical study of the solute dispersion in microchannel with interphase transport

Wenbo Li[1]*, Wenyao Zhang[1], Huang Deng[1], and Qian Fang[1], Cunlu Zhao[1]†

[1] Key Laboratory of Thermo-Fluid Science and Engineering of MOE, Xi'an Jiaotong University, Xi'an 710049, Shaanxi, P.R. China

*Presenting author: wenboli817@gmail.com

†Corresponding author: mclzhao@xjtu.edu.cn

Abstract

The dispersion phenomenon in the pressure-driven microchannel flow of solute with interphase transport is numerically studied using a transient 2D model. The interphase mass transport between the mobile phase and the stationary phase of the microchannel plays a critical role in the process of solute dispersion. The traditional studies of the solution dispersion with the interphase transport are based on the moment analysis which actually uses the 1D model and cannot provide detailed understandings of the solute dispersion in the microchannel. In this work, the 2D numerical model enables a more detailed characterization of the transient evolution of the solute dispersion in a microchannel by predicting the 2D transient concentration contours of the solute. The model characterizes the effect of interphase mass transport on the solute dispersion with two parameters, i.e., the partition coefficient (K) and the kinetic mass transfer rate (k_f). From the 2D concentration contours, we observe that the solute is more dispersed in the mobile phase along the microchannel axis and also moves slower with K increasing, which indicates significant dispersion and retention of solute in the microchannel respectively. For a smaller k_f which means a high mass transfer resistance between the mobile and stationary phases, the solute concentration in mobile phase is more dispersed and also the corresponding concentration profile along the channel axis is more skewed. It is also noticed that a thicker layer of stationary phase (d_f) corresponding to a larger solute capacity of the stationary phase, causes more significant retention of solute in the microchannel. The results from this study provide a straightforward picture of the solute dispersion phenomenon in microchannel with interphase transport and are of high relevance to practical applications such as chromatography and microfluidics.

Keywords: Microchannel; Dispersion; Interphase Transport; Concentration Contour

Introduction

With the rapid development of microfluidic lab-on-a-chip (LOC) technology, study of fluids and solute transport in microchannels have received widespread attention since miniaturization of fluid channels in microfluidic LOC devices leads to new problems for the fluid and mass transport. The dispersion of solutes in fluids flows in microchannels is one of the most widely studied topic due to its key roles in the trace detection of samples, chromatography, multiphase microfluidics and soil remediation[1-3], etc.

The study of solute dispersion has been a constant focus since Taylor who investigated analytically and experimentally the solute dispersion in the water flowing in a tube due to the hydrodynamic convection and molecular diffusion [4-6]. Basing on Taylor's studies, Aris [7] presented a theoretical study of the solute dispersion by means of moments analysis. The works by Taylor and Aris form the theoretical basis for the solution dispersion, their approach is jointly termed as the Taylor-Aris theory. Later Aris studied the solute dispersion in two coaxial layers of immiscible fluids flowing in an annulus. In addition to the traditional solution dispersion mechanisms of hydrodynamic convection and molecular diffusion, the interphase exchange between two fluids was also taken into account as a new mechanism. The consideration of this new mechanisms is due to a number of applications such as distillation and partition chromatography in which interphase mass transport has a crucial contribution [8]. In such researches, moments are adopted as the theoretical tool because of their ability in providing good statistical descriptions of the solute concentration distribution in the term of time. Kučera [9] derived explicit moments expressions as part of his study on non-equilibrium chromatography considering the longitudinal diffusion in the mobile phase, the radial diffusion inside the porous grains of the packing material, the finite rate of mass transfer through the boundary. Grushka [10] related the moments of a chromatographic peak to the determinative experimental parameters, i.e., partition coefficients, column length, etc. J. A. Jonsson proposed that considering the solute dispersion, the median of the chromatographic peak should be taken as the best measurement of retention time[11] and gave the moments to specifically study the dispersion and to determine the isotherm[12]. The moment analysis not only provides insightful understanding of fundamental characteristics of solution dispersion in channel flows, but also is practically useful in determining the diffusivity of solutes in specific solutions and the partition coefficient of solute between two phases [13-16] by the inverse chromatography.

Another popular method to study solute dispersion in microchannel flow is based on the concept of height equivalent to a theoretical plate (H.E.T.P.) [17-19]. Different from the moment analysis which focuses only on the statistical description of solution dispersion on time scale, H.E.T.P describes the instant equilibrium of solution dispersion on length scale. The introduction of H.E.T.P to the solute dispersion study is due to its wide use as an indicator for separation performance in the chromatography. Various investigations performed fundamental study of the solution dispersion in chromatography using the H.E.T.P. and particularly discussed the effects of various factors, such as solute diffusivity and phase ratio, on the

H.E.T.P. [20-22]. Fabrice presented a comprehensive summary for the solution dispersion studies based on the H.E.T.P. in the field of chromatography [23]. Recently, Beauchamp investigated the solute dispersion in both short and long capillary with the H.E.T.P under the slip boundaries and reached the conclusion that only in tube of very small diameters the use of slip flow boundary to reduce chromatography dispersion is suitable [24].

The aforementioned moment analysis and H.E.T.P methods focus on different aspects of the solute dispersion, but are all the simplified models of the more general convection-diffusion theory of mass transport. As has been reviewed previously, there has been significant development in the moment analysis and H.E.T.P. for investigating solute dispersion. Yet, these two methods are derived from the general convection-diffusion theory with a cross-section average treatment, and thus cannot provide detailed information of the solute concentration distribution in the whole channel domain. Especially, the details of the solute exchange between two phases (mobile phase and stationary phase) are missing from these simplified models. The present work is to study the solute dispersion in a pressure-driven microchannel flow with interphase transport with a full numerical model based on the convection-diffusion theory. The model is able to give an intuitive understanding of the solution transport with the numerically predicted transient concentration contours in the microchannel. More interestingly, the interphase transport of solute is to be studied in an unprecedented detail. Our numerical analyses also systematically address the effects of various model parameters on the solution dispersion characteristics.

Methods

Mathematical model

Considering a circular straight microchannel whose inner wall holds an extremely thin layer of static polymer liquid, gases flow in the microchannel without causing the flow of liquid. The gases are termed as the mobile phase and the polymer liquid as the stationary phase.

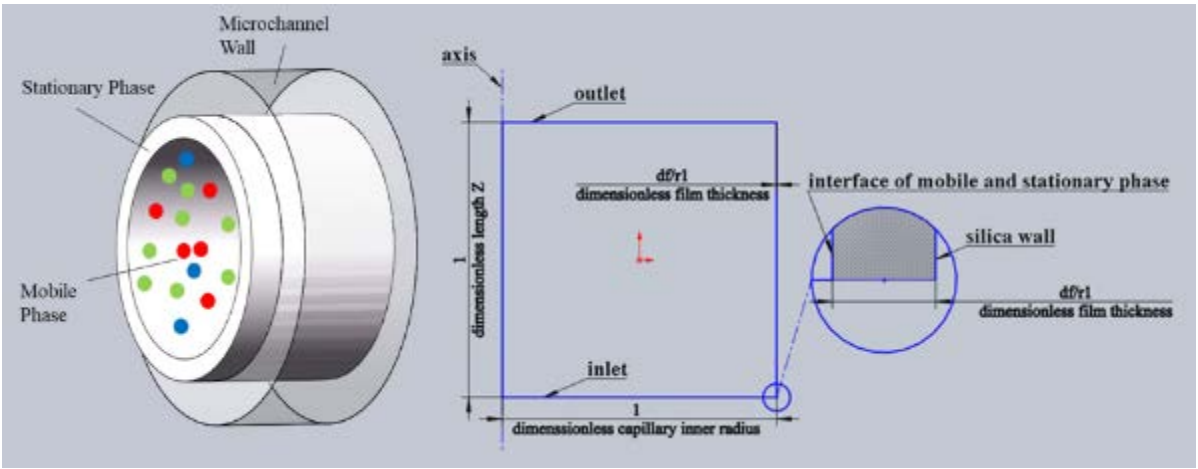

Figure 1. Schematic of physical model and computational domain

The physical model and the corresponding computational domain of this study are showed in figure 1. The mobile phase is mixed of the carrier gas inert to the stationary phase and the injected gaseous solute. In this study, the mobile phase is incompressible and under isothermal condition. The diffusions along both axial and radial conditions are considered and the diffusivities of solute in both mobile and stationary phase are concentration independent. The stationary phase is homogenous and has constant thickness along axial direction of the microchannel. What's more, no chemical reaction occurs during the flow through the microchannel. Due to the magnitudes of the diameter and the flow rate in microchannel, the velocity distribution of mobile phase obeys Poiseuille's law. Considering that the solute is dilute, the mass convection-diffusion equation is only performed on solute. Based on above assumptions and equations from results of Aris[8], and with dimensionless parameters introduced as following,

$$c_m = \left(\frac{c_1}{c_0}\right) \quad Z = \left(\frac{z}{L}\right) \quad c_s = \left(\frac{c_2}{c_0}\right) \quad T = \left(\frac{U_1 t}{L}\right) \quad R = \left(\frac{r}{r_1}\right)$$

the dimensionless PDEs, I.C. and B.C.s of this study are:

$$\frac{\partial c_m}{\partial T} + 2[1-R^2]\frac{\partial c_m}{\partial Z} = \frac{h_0}{Pe_1}\frac{1}{R}\frac{\partial}{\partial R}\left(R\frac{\partial c_m}{\partial R}\right) + \frac{1}{Pe_1 h_0}\frac{\partial^2 c_m}{\partial Z^2} \qquad 0 < R < 1 \tag{1}$$

$$\frac{\partial c_s}{\partial T} = \frac{h_0}{Pe_2}\frac{1}{R}\frac{\partial}{\partial R}\left(R\frac{\partial c_s}{\partial R}\right) + \frac{1}{Pe_2 h_0}\frac{\partial^2 c_s}{\partial Z^2} \qquad 1 < R < \frac{r_1 + d_f}{r_1} \tag{2}$$

Initial condition is set that no solute is in microchannel before injection:

$$c_m(R,Z,T) = c_s(R,Z,T)/K = 0 \qquad at\ T = 0, 0 < Z < 1 \tag{3}$$

At the inlet of the microchannel, the Dirac delta function is adopted to express the instantaneously uniform injection.

$$c_m(R,Z,T) = \frac{U_1}{L}\delta(T) \qquad at\ Z = 0 \tag{4}$$

At the interface of the mobile and the stationary phases, a kinetic equation is used to govern the interphase transport complying with the mass conservation law. The direction of interphase transport is decided by the value of c_m-c_s/K. The partition coefficient, K, physically brings solute to bear a linear limit concentration relationship between the mobile phase and the stationary phase. K_f represents the dimensionless mass transport rate at the interface of the mobile and the stationary phase. When K_f goes infinite the boundary condition (5) degenerates to the ideal one[14].

$$\frac{h_0}{Pe_1}\frac{\partial c_m}{\partial R} = \frac{h_0}{Pe_2}\frac{\partial c_s}{\partial R} = -K_f(c_m - c_s/K) \qquad at\ R = 1 \tag{5}$$

Symmetric condition is set at the axis of microchannel.

$$\frac{\partial c_m}{\partial R} = 0 \qquad at\ R = 0 \tag{6}$$

And no reaction or adsorption occurs between solute and microchannel wall.

$$\frac{\partial c_s}{\partial R} = 0 \qquad at\ R = \frac{r_1 + df}{r_1} \tag{7}$$

where r_1 is the inner radius and L the length of microchannel and d_f is the thickness of the stationary phase. c_0 is the injection concentration of the solute and U_1 the mean velocity of the mobile phase. The concentrations are c_1 and c_2 while the diffusivities of solute are D_1 and D_2, respectively in the mobile phase and the stationary phase.

The definition of dimensionless parameters are $Pe_1=r_1u_1/D_1$, $Pe_2=r_1u_1/D_2$, $K_f = k_f t_0/r_1$, $h_0=L/r_1$, where $t_0=L/U_1$represents the time for carrier gas to flow through the microchannel. Here one should distinguish the Peclet number Pe_1 from Pe_2 which only takes the symbol of Peclet number, and the physically meaning of Pe_2 is the ratio of the convection in the mobile phase over the solute diffusivity in the stationary phase.

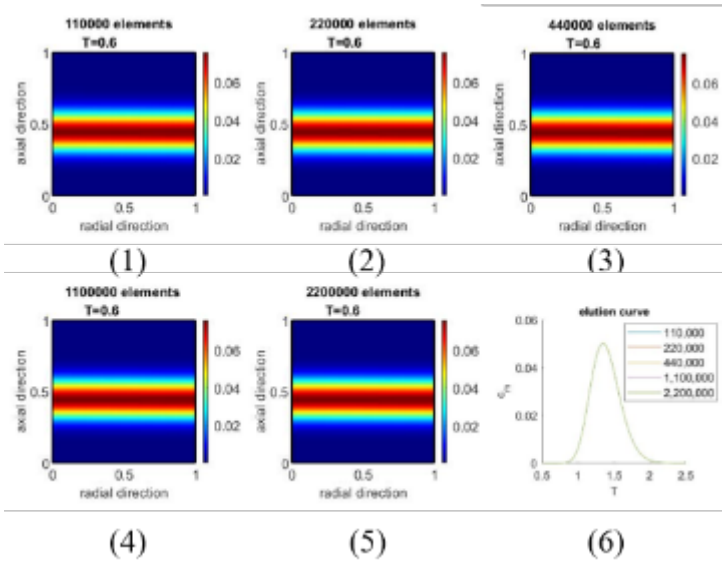

Figure 2. Mesh independence verification

Model verification

The finite element method is adopted for the computation operated by COMSOL Multiphysics 5.4 in this study. The mesh is constructed quadrilateral in the computational domain in figure 1. The distribution of mesh elements is symmetry in both axial and radial directions while near the interface of the mobile and the stationary phase the mesh is more compact. To conduct a

transient computation, the relative tolerance in solver is set 0.001 with respect to time. Figure 2 shows the verification of mesh independence with varying total mesh elements from 110,000 to 2,200,000. From the contours and the concentration profile in terms of time at the outlet of the microchannel, namely, the elution curve, of different cases, the mesh independence is verified. We take 1,100,000 as the number of mesh elements to perform computation and set $t_0 = 40,\ h_0 = 100$ constant in all the computational cases. Values of other parameters are set based on practicability. Pawlisch[14] once gave a computational result in his paper and we recurred his result with the 1-D model as the reference. Then we computed the dimensionless 2-D model before-mentioned under the same condition of Pawlisch's result for contrast. The results and comparation are shown in figure 3. The picture shows good agreement of two models indicating that the dimensionless 2-D model is correct.

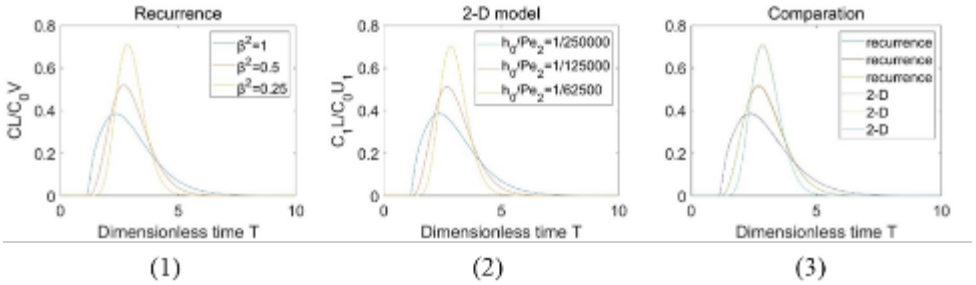

Figure 3. Verification of proposed 2-D model by Recurrence of Pawlisch's Case

Results and discussion

Solute dispersion in microchannel with interphase transport is affected by three simultaneous process, i.e., the hydrodynamic convection/molecule diffusion in the mobile phase[4], the molecule diffusion in stationary phases and the interphase transport between the two phases[8]. The discussion in this section consists of three subsections. In the first subsection, we show the general influence of interphase transport by comparing the concentration contours of solute dispersion with and without interphase transport. In the second subsection, we use concentration distribution contours to illustrate the impact of Pe_1 and Pe_2 on dispersion. In the third section, we discuss the influence of K, K_f and d_f/r_1 on dispersion. In all figures of contours shown below, the time-varying contours of the same parameter are placed in the same row while the parameter-varying contours of the same time are placed in the same column.

Dispersion with interphase transport

In this subsection, impacts of interphase transport on solute dispersion is discussed without loss of generality. Figure 4 shows two series of contours of which (a) is related to the solute dispersion without interphase transport and (b) is related to the solute dispersion with interphase transport. The two cases share the same parameters that $Pe_1 = 100$ while only the case (b) has a set of parameters, i.e., $Pe_2 = 10000, K = 100, K_f = 10^6$. It should be noted here that the value of K_f indicates extremely large rate of interphase transport which can be regarded that

$c_m = c_s$ is tenable at the interface of two phases all along. The contours show clearly that interphase transport results in the enhancement of solute dispersion and solute retention in microchannel.

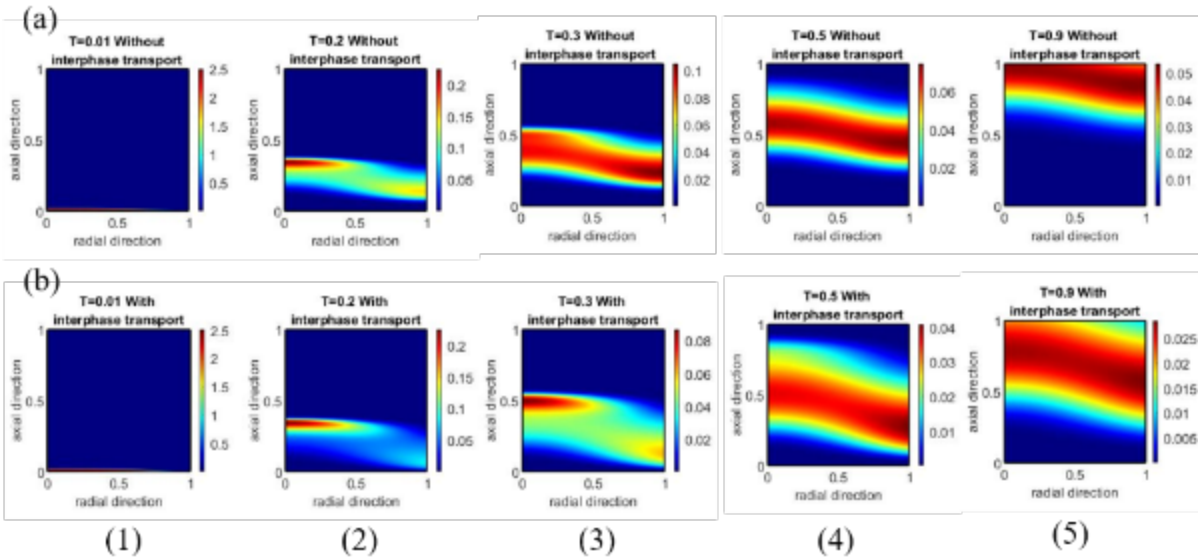

Figure 4. Contrast contours of solute dispersion without and with interphase transport

At the inlet of the microchannel, injected solute is not dispersed yet (a1, b1). With the proceeding of flow, the Poiseuille's law acts on the solute that a parabolic but uneven concentration distribution can be observed in (a2) and (b2) whose contours in main stream are almost the same. However, solute dispersion caused by interphase transport show up that the solute concentration is smaller and the concentration distribution band is wider in (b2) near the interface than that in (a2) near the wall. The concentration gradient near the wall decreases slowly compared to that in the main stream thus a concentration gradient pointing from the wall to the main stream formed as shown in (a3). The diffusion of solute into the stationary phase causes the decrease of solute concentration in the mobile phase near the interface since with a Pe_1 equals 100, diffusion in mobile phase is not strong enough to compensate the depletion of solute into the stationary phase. Consequently, the solute is more dispersed and the transport of solute into the stationary phase delays the formation of concentration band in the mobile phase with the contrast of (a3) and (b3). The concentration band is more even and narrower in (a4) than that in (b4). Once the parabolic solute concentration band is formed, longitudinal concentration gradient becomes significant thus the dispersion evolves broader in axial direction till the outlet of the microchannel as shown in (a5) and (b5). However, the concentration band in (b5) moves much slower and is also wider than the band in (a5). In sum, the existence of interphase transport causes the solute moves with a smaller velocity and disperses much stronger in the microchannel.

Impacts of Pe_1 and Pe_2

The radial motion of solute consists of three parts, i.e., diffusion in the mobile and the stationary phases and the interphase transport. The direction of solute radial motion is controlled by the difference of solute concentrations at the interface between the mobile phase and the stationary phase, namely, the value of c_m-c_s/K. Each of the three parts has a resistance to solute diffusion[25]. Based on the mass conservation law, the solute diffusion from one phase to the other is analogous to the electric current through three tandem different resistances. We set $K = 100, K_f = 10^6$ (infinitely large interphase transport rate) to investigate the impacts of Pe_1 and Pe_2 on the solute dispersion.

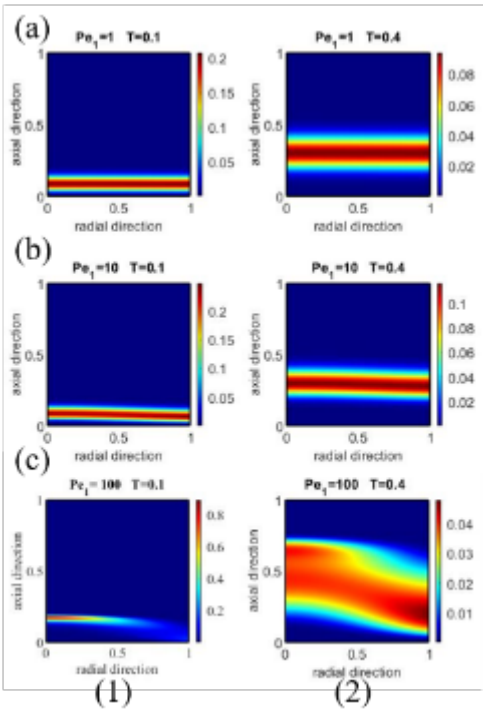

Figure 5. Concentration distribution contours of solute with different Pe_1

Firstly, figure 5 shows the concentration contours of different Pe_1 with Pe_2=10^5. In row (a1) and (b1), the concentration band is of plug shape. In (c1) Pe_1 equals 100, the concentration band is of parabolic shape. This is the evidence of solute dispersion by a stronger convection. Since the impact of diffusivity in the mobile phase will appear later with increase of Pe_1, the concentration band is narrower and more bent in column (1). Later with the proceeding of flow the concentration band reforms dramatically wide in the case of Pe_1=100. The concentration bands in (a2) and (b2) keep their shape and moves with weaker dispersion. Consequently, a much small or much big Pe_1 will both cause a stronger solute dispersion while a much big one is worse for the trace detection. It takes longer with larger Pe_1 for diffusion in the mobile phase to compensate the depletion of solute due to interphase transport into the stationary phase and thus the reformation of concentration band is slower and the reformed band is dramatically

wide. This indicates an optimal concentration Pe_1 to be chosen which is consistent with the result of H.E.T.P.[17] to choose an optimal flow rate.

Secondly, Figure 6 gives a comparation of the solute dispersion of different Pe_2 and constant Pe_1=100. It can be seen from (1) and (2) that with increasing of Pe_2 from 10^5 to 10^6, the concentration band has little difference. However, with increasing of Pe_2 from 10^6 to 10^7, the concentration band is wider and one can observe a relatively high concentration in mainstream (3) rather than near the interface (2). The big Pe_2 indicates a relatively slow diffusion in the stationary phase so it takes longer for solute to change the diffusion direction from into the stationary phase to out of the stationary phase. Additionally, in (3) the concentration distribution is wider at the upstream of the most concentrated part than that at the downstream. This is because that the point satisfying $c_m=c_s/K$ moves upstream as a result of the big Pe_2. In sum, the change of Pe_2 below 10^6 has neglectable influence on solute dispersion while increasing of Pe_2 from 10^6 to 10^7 causes a stronger solute dispersion and an asymmetric concentration distribution. This can be verified by the elution curve shown in figure 7.

Figure 8 shows a series of solute concentration contours ordered chronologically with Pe_1=100 and $Pe_2=10^7$. The contours in the enlargement part of figures are depicted with the replacement of c_s by c_s/K for sake of observation. As aforementioned, Pe_2 is the ratio of the convection in the mobile phase over the solute diffusivity in the stationary phase. Due to a big Pe_1, when T=0.1 the solute flows in the mobile phase with a parabolic but uneven distribution as shown in the contour (1) and the concentration of the solute left in the stationary phase is satisfied with the relationship $c_m<c_s/K$. In other words, this part of solute is lagged by the stationary phase. When the concentration band forms as shown in (2), the solute diffuse into the stationary phase at the downstream where $c_m>c_s/K$ and out of the stationary phase at the upstream where $c_m<c_s/K$. This indicates that there would be a point satisfying the condition $c_m=c_s/K$. With the proceeding of flow, the concentration band broadens and the difference of c_m and c_s/K vanishes gradually as shown in (3) and (4). By far, the process of solute dispersion with interphase transport has been clearly illustrated.

Impacts of K, K_f and d_f/r_1

This subsection will discuss the impacts of K, K_f and d_f/r_1 with $Pe_2=10^5$. The partition coefficient, K, indicates the limit of interphase transport and the dimensionless kinetic mass transfer rate, K_f, represents the ratio of interphase transport rate over the diffusion rate in terms of r_1/t_0. Both of the two parameters characterize the interphase transport. The ratio of d_f over r_1 represents the relative thickness of the stationary phase. With a constant diffusion rate in the stationary phase, it takes longer time to reach an even radial distribution in the stationary phase under the condition of a larger d_f/r_1.

Firstly, figure 9 shows the contours of different K with Pe_1=1 and $K_f=10^6$. With K increasing from 100 in row (a) to 400 in row (d), the concentration band moves slower gradually. The

solute velocity is proportional to the fraction of solute in the mobile phase[26]. As a result, the solute with a larger K will be retained in the microchannel longer. Solute diffuses into the stationary phase more with the K increasing.

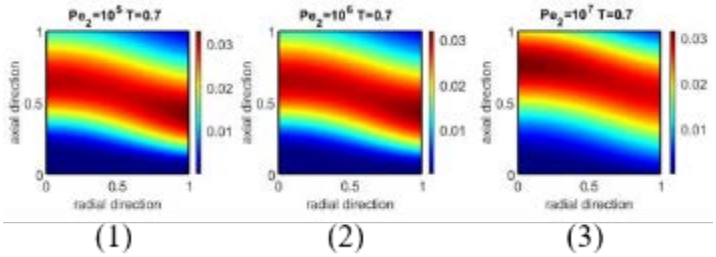

Figure 6. Concentration distribution contours of solute with different Pe_2

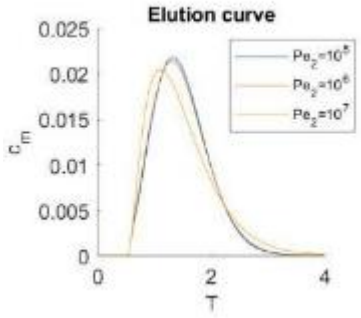

Figure 7. Elution curve of solute with different Pe_2

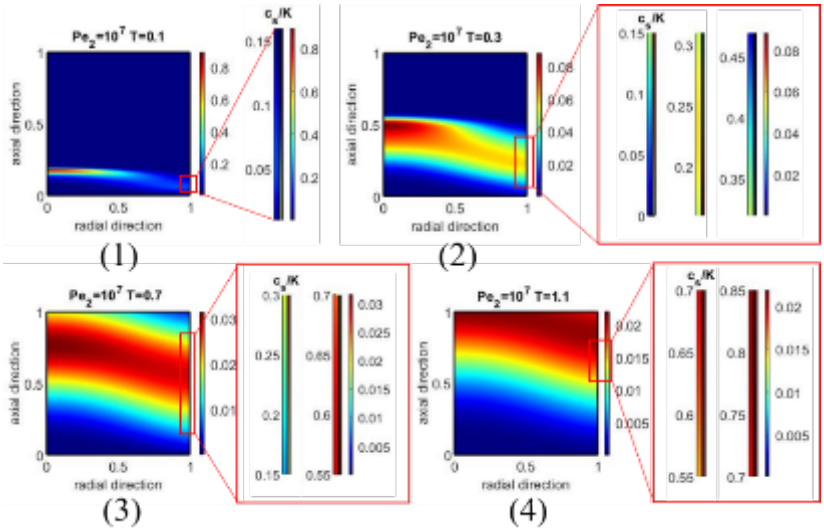

Figure 8. Evolution concentration contours of solute dispersion with Pe_2=10^7

Consequently, the solute velocity in the mobile phase decreases thus the solute band in the stationary phases get wider. The wider band in stationary phase causes a wider solute concentration band in the mobile phase. In sum, solute of stronger affinity to the station phase, namely, larger partition coefficient K, will be dispersed wider and stay longer in the

microchannel. This can be verified by the elution curve in Figure 10(1). Partition coefficient is the key factor that makes solutes separation in microchannel feasible.

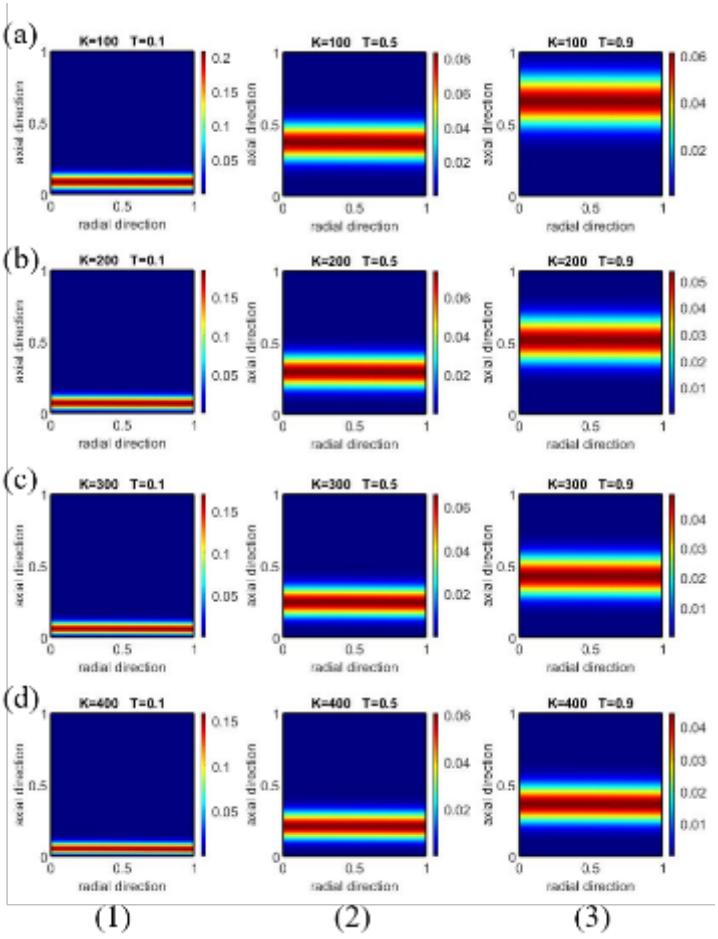

Figure 9. Concentration distribution contours of solute with different K

Secondly, figure 11 shows the concentration contours of solute of different K_f with Pe_1=1 and K=100. In this study $K_f = k_f t_0/r_1$, we assume t_0 and r_1 constant to specifically investigate the impact of k_f on the solute dispersion. From the enlargement part of contours in column (1), it can be observed that with increase of K_f, the difference between c_m and c_s/K goes smaller. In column (2) with K_f increasing from 1.6 to 160, the solute concentration band becomes narrower but the band widths of (a2) and (b2) differs to a larger extent than those of (b2) and (c2). However, the solute concentration band in (c2) and (d2) have few differences in width and value. In addition, (a2) tells that a small K_f causes the asymmetry of solute concentration band with respect to the most concentrated point. However, the change of K_f does not cause the change of the retention time of solute in microchannel. This can be verified by the elution curve in figure 10 (2). The combinative function of K and K_f results in the retention and asymmetric solute dispersion in the microchannel. As aforementioned, there would be an ideal point satisfying $c_m=c_s/K$ at the interface. Solute diffuses into the stationary phase at the downstream ($c_m>c_s/K$) of the ideal point while the solute diffuses out of the stationary phase at the upstream of the ideal point. The position of the ideal point is the most concentrated point of solute band

under the ideal condition, namely, K_f is infinitely large. Under the real condition that K_f is finite, the ideal point moves to the upstream of the most concentrated point.

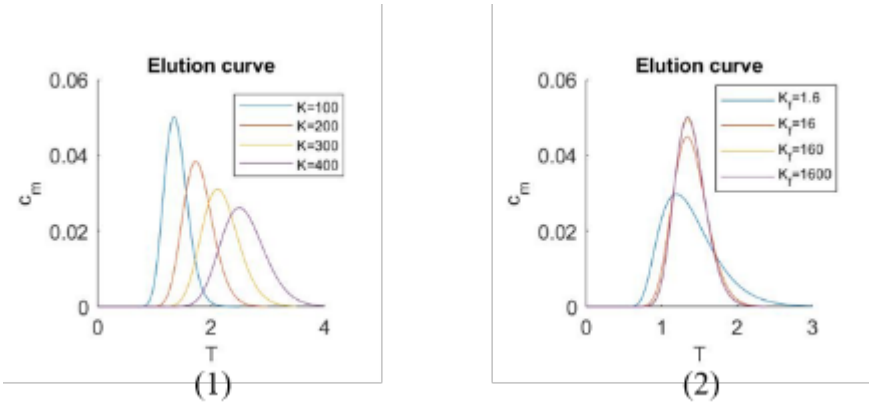

Figure 10. Elution curves of different K in (1) and of different K_f in (2)

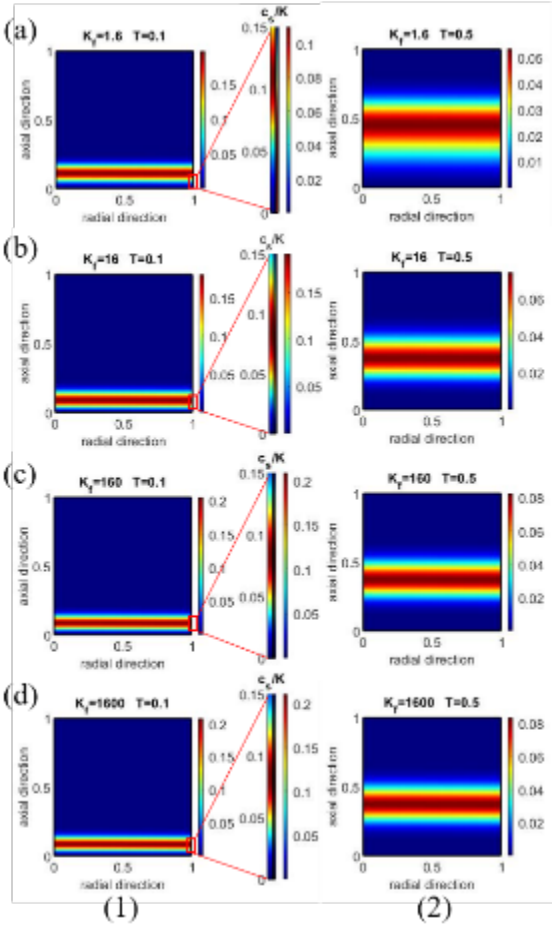

Figure 11. Concentration distribution contours of solute with different K_f

In the other word, the condition, $c_m=c_s/K$, at the interface is delayed thus the diffusion of solute out of the stationary phase is delayed. Consequently, the solute concentration band is tailed at the upstream and the elution curve is left-leaning as shown in figure 10 (2). In sum, for a smaller K_f which means a high mass transfer resistance between the mobile and stationary phases, the solute is more dispersed in the mobile phase and also the corresponding concentration band

becomes asymmetric. As K_f is beyond 160, the further increase of K_f affects the solute dispersion marginally.

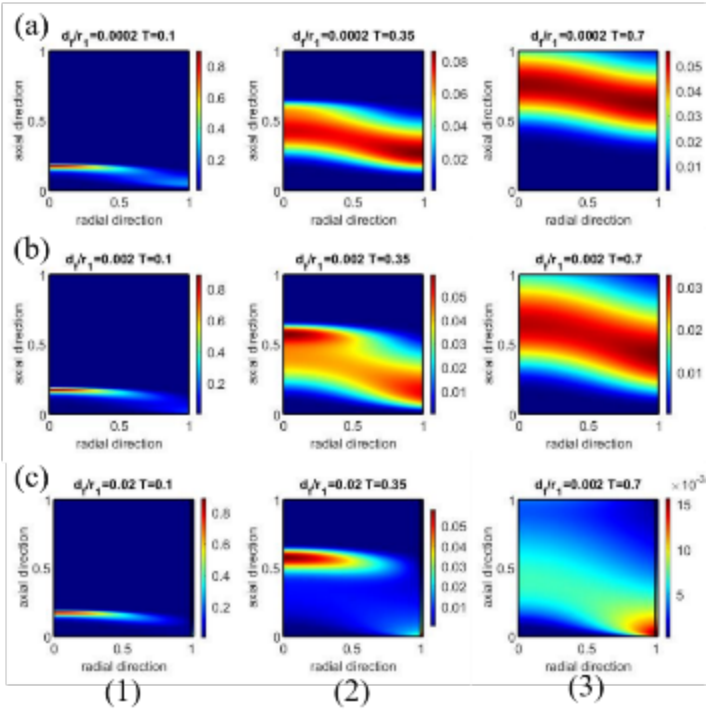

Figure 12. Concentration distribution contours of solute with different d_f/r_1

Thirdly, figure 12 shows the concentration contours of solute of different d_f/r_1 with Pe_1=100 and K_f=1600. We assume r_1 constant to specifically investigate the influence of d_f. In column (1) when the solute dispersion is mainly caused by convection, the solute concentration in mobile phase near the interface increases as d_f/r_1 decreases. And when the solute band forms, the solute concentration band goes wider as d_f/r_1 increases from 0.0002 of (a2) to 0.002 of (b2). However, the band in (c2) is far from formation due to the extremely strong retention of solute caused by relatively thick stationary phase. Additionally, in (a2) according to the contour the solute has begun to diffuse out of the stationary phase while in (b2) not yet. Contours show that at the same dimensionless time T=0.7, when the concentration are distributed evenly, the most concentrated point of solute band in (b3) is further from the outlet of the microchannel than that of solute band in (a3). Consequently, the increase of the d_f/r_1 also causes the delay of solute from flow out of the microchannel. This is consistent with the mathematical expression of the first moment[14]. However, in (c3) the solute in main stream has flow out of the microchannel, which indicates that with a relatively thick stationary phase, the retention of solute is so strong that the solute band is not formed in the microchannel. In sum, as d_f/r_1 increases the solute capacity of the stationary phase increases and consequently, on one hand the solute is more significantly retained in the microchannel, but on the other hand the solute band may be not able to form in the microchannel.

Conclusions

A transient 2-D numerical model based on the convection-diffusion theory is formulated to study the solute dispersion in pressure-driven microchannel flow with the interphase transport. The solute dispersion in the mobile phase is shown to be affected by three processes, i.e., the hydrodynamic convection/molecule diffusion in the mobile phase, the molecule diffusion in stationary phases and the interphase transport between the two phases. In the present analysis, various nondimensional parameters are defined to facilitate the discussion of effects of the three processes on the solution dispersion. Specifically, Pe_1 represents the combined effect of hydrodynamic convection and molecule diffusion in the mobile phase, Pe_2 represents the effect of molecule diffusion in stationary phase, K and K_f represent the effect of interphase transport.

From the 2D transient concentration contours, we observe that with increase of Pe_1 from 1 to 10, the solute concentration band becomes narrower and bent slightly. With the Pe_1 further increasing to 100, and the concentration band becomes extremely irregular. As Pe_2 is below 10^6, Pe_2 has negligible effect on the solute dispersion. However, with the increase of Pe_2 from 10^6 to 10^7, the solute shows a significant increase of dispersion in mobile phase. With K increasing from 100 to 400, the solute becomes more dispersed in the mobile phase along the microchannel axis and also shows prolonged retention in the microchannel. For a smaller K_f which means a high mass transfer resistance between the mobile and stationary phases, the solute is more dispersed in the mobile phase and also the corresponding concentration band becomes asymmetric. As K_f is beyond 160, the further increase of K_f affects the solute dispersion marginally.

It is also noticed that a thicker layer of stationary phase (d_f) corresponding to a larger solute capacity of the stationary phase, on one hand causes a more significant retention of solute in the microchannel, but on the other hand leads to no formation of the solute band.

References

[1] Chakraborty, D., Bose, N., Sasmal, S., Dasgupta, S., Maiti, T. K., Chakraborty, S., et al. (2012) Effect of dispersion on the diffusion zone in two-phase laminar flows in microchannels, *Analytica Chimica Acta*, **710**, 88-93.

[2] Datta, S., and Ghosal, S. (2009) Characterizing dispersion in microfluidic channels, *Lab Chip*, **9**, 2537-2550.

[3] Wang, P., and Chen, G. Q. (2016) Solute dispersion in open channel flow with bed absorption, *Journal of Hydrology*, **543**, 208-217.

[4] Taylor, G. (1953) Dispersion of soluble matter in solvent flowing slowly through a tube, *Proceedings of the Royal Society of London. Series A, Mathematical and Physical Sciences*, **219**, 186-203.

[5] Taylor, G. (1954) The Dispersion of Matter in Turbulent Flow through a Pipe, *Proceedings of the Royal Society of London. Series A, Mathematical and Physical Sciences*, **223**, 446-468.

[6] Taylor Geoffrey, I. (1954) Conditions under which dispersion of a solute in a stream of solvent can be used to measure molecular diffusion, *Proceedings of the Royal Society of London. Series A. Mathematical and Physical Sciences*, **225**, 473-477.

[7] Aris, R. (1956) On the dispersion of a solute in a fluid flowing through a tube, *Proceedings of the Royal Society of London. Series A. Mathematical and Physical Sciences*, **235**, 67-77.

[8] Aris, R., and Taylor Geoffrey, I. (1959) On the dispersion of a solute by diffusion, convection and exchange between phases, *Proceedings of the Royal Society of London. Series A. Mathematical and Physical Sciences*, **252**, 538-550.

[9] Kučera, E. (1965) Contribution to the theory of chromatography: Linear non-equilibrium elution chromatography, *Journal of Chromatography A*, **19**, 237-248.

[10] Grushka, E. (1972) Chromatographic peak shapes. Their origin and dependence on the experimental parameters, *The Journal of Physical Chemistry*, **76**, 2586-2593.

[11] Jonsson, J. A. (1981). *The median of the chromatographic peak as the best measure of retention time* (Vol. 14).

[12] Jaulmes, A., Vidal-Madjar, C., Gaspar, M., and Guiochon, G. (1984) Study of peak profiles in nonlinear gas chromatography. 2. Determination of the curvature of isotherms at zero surface coverage on graphitized carbon black, *The Journal of Physical Chemistry*, **88**, 5385-5391.

[13] Tihminlioglu, F., and Danner, R. P. (1999) Application of inverse gas chromatography to the measurement of diffusion and phase equilibria in polyacrylate–solvent systems, *Journal of Chromatography A*, **845**, 93-101.

[14] Pawlisch, C. A., Macris, A., and Laurence, R. L. (1987) Solute diffusion in polymers. 1. The use of capillary column inverse gas chromatography, *Macromolecules*, **20**, 1564-1578.

[15] Ronco, N. R., Menestrina, F., Romero, L. M., and Castells, C. B. (2019) Determination of gas–liquid partition coefficients of several organic solutes in trihexyl (tetradecyl) phosphonium dicyanamide using capillary gas chromatography columns, *Journal of Chromatography A*, **1584**, 179-186.

[16] Navarro-Tovar, G., Moreira, J., Valades-Pelayo, P., and Lasa, H. (2014). *Diffusion and Equilibrium Adsorption Coefficients of Aromatic Hydrocarbon Species in Capillary Columns* (Vol. 12).

[17] Giddings, J. C. (1961) Plate Height Contributions in Gas Chromatography, *Analytical Chemistry*, **33**, 962-963.

[18] Giddings, J. C. (1962) Plate Height Theory of Programmed Temperature Gas Chromatography, *Analytical Chemistry*, **34**, 722-725.

[19] Giddings, J. C. (1962) Liquid Distribution on Gas Chromatographic Support. Relationship to Plate Height, *Analytical Chemistry*, **34**, 458-465.

[20] Frey, G. L., and Grushka, E. (1996) Numerical Solution of the Complete Mass Balance Equation in Chromatography, *Analytical Chemistry*, **68**, 2147-2154.

[21] van Deemter, J. J., Zuiderweg, F. J., and Klinkenberg, A. (1995) Longitudinal diffusion and resistance to mass transfer as causes of nonideality in chromatography, *Chemical Engineering Science*, **50**, 3869-3882.

[22] Knox, J. H. (2002) Band dispersion in chromatography—a universal expression for the contribution from the mobile zone, *Journal of Chromatography A*, **960**, 7-18.

[23] Gritti, F., and Guiochon, G. (2012) Mass transfer kinetics, band broadening and column efficiency, *Journal of Chromatography A*, **1221**, 2-40.

[24] Beauchamp, M. D., and Schure, M. R. (2019) Simulation and theory of open-tube dispersion in short and long capillaries with slip boundaries and retention, *Journal of Chromatography A*, **1588**, 85-98.

[25] Khan, M. A. (1960) Non-Equilibrium Theory of Gas-Liquid Chromatography, *Nature*, **186**, 800-801.

[26] Giddings, J. C. (1965). *Dynamics of Chromatography*.